IOP Publishing | Astro Ltd
Laser Physics Letters
Laser Phys. Lett. **11** (2014) 106001 (5pp)
doi:10.1088/1612-2011/11/10/106001

Laser control of filament-induced shock wave in water

F V Potemkin, E I Mareev, A A Podshivalov and V M Gordienko

Faculty of Physics and International Laser Center M.V. Lomonosov Moscow State University, Leninskie Gory, bld.1/62, 119991, Moscow, Russia

E-mail: potemkin@automationlabs.ru

Received 6 May 2014, revised 21 July 2014
Accepted for publication 14 August 2014
Published 5 September 2014

Abstract

We discovered that tight focusing of Cr:forsterite femtosecond laser radiation in water provides the unique opportunity of long filament generation. The filament becomes a source of numerous spherical shock waves whose radius tends to saturate with the increase of energy. These overlapping waves create a contrast cylindrical shock wave. The laser-induced shock wave parameters such as shape, amplitude and speed can be effectively controlled by varying energy and focusing geometry of the femtosecond pulse. Aberrations added to the optical scheme lead to multiple dotted plasma sources for shock wave formation, spaced along the optical axis. Increasing the laser energy launches filaments at each dot that enhance the length of the entire filament and as a result, the shock impact on the material.

Keywords: femtosecond filament, laser-induced shock waves, aberrations

(Some figures may appear in colour only in the online journal)

1. Introduction

The propagation of an intense, focused femtosecond laser pulse in optically transparent condensed matter is accompanied by numerous complicated processes taking place inside the medium. At laser intensities above $I \sim 10^{12}\,\mathrm{W\,cm^{-2}}$ the main roles played are linear and nonlinear absorption, Kerr self-focusing and plasma defocusing. Therefore, due to a dynamic balance between self-focusing, plasma defocusing and diffraction, when the peak power of the laser pulse (P_l) exceeds the critical power (P_{cr}), a laser filament is fired in the medium [1] and the laser-induced shock wave can spread around the plasma channel. Parameters of the laser-induced shock wave strongly depend on the specific energy delivery. Due to this reason, it can be expected that in a tight-focusing regime it is possible to build an extreme state of matter. If the beam aperture is quite large and $P_l >> P_{cr}$, multifilamentation occurs. Additionally, the power conserved in the each filament is about P_{cr}, thus energy is distributed between the filaments and the energy reservoir is stretched out over a huge area [1]. The tight focusing of the laser beam can sufficiently increase the laser pulse intensity in the irradiated area (up to $I \sim 10^{14}\,\mathrm{W\,cm^{-2}}$ [2–5]). Thus, Kerr self-focusing prevails over plasma defocusing and diffraction and one continuous plasma channel can thereby be formed. A similar effect has also been observed in gases [6]. Moreover, at such high laser intensities, high-order processes may start to play a significant role that, in turn, complicates the scenario of laser-matter interaction. The nonlinear refractive index also can be efficiently changed by molecular vibrations and librations, which are excited by resonant laser–matter interactions [7]. It should be stressed that currently there are few studies that describe propagation of an intense femtosecond pulse tightly focused into liquids accompanied by filament formation and various post-effects on nanosecond and microsecond timescales [1, 8]. There are several studies describing the shock waves induced by the femtosecond filament in crystalline transparent dielectrics [9, 10] but the absence of the crystal lattice leads to different routes in laser energy redistribution, which, in turn, reflects on the nature of laser-induced shock wave generation and evolution [11].

The main carriers of laser energy to matter are plasma electrons. The amount of energy delivered to the medium depends on the density of electrons and their mean energy. Plasma electron densities achieved in a tight focusing geometry ($n_e \sim 10^{20}\,\mathrm{cm^{-3}}$) are much higher than in the case of collimated or loosely focused beams ($n_e \sim 10^{18}\,\mathrm{cm^{-3}}$) with the same energy [12, 13]. Hence, in a tight focusing geometry,

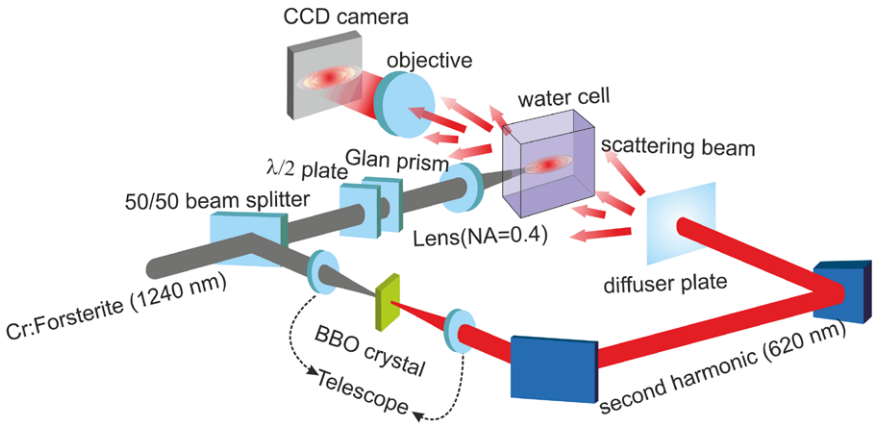

Figure 1. Experimental setup. The incoming femtosecond laser pulse splits into two channels. The pump pulse is tightly focused by aspheric lens into the water cell. The energy of pump pulse is varied by a half-wave plate and a Glan prism. The second harmonic is used as a probe pulse and is scattered in a matted plate. After it is passed through the water cell with a shock wave, the probe radiation is collected by microscope objective on the CCD matrix. The temporal resolution of this scheme is about 200 fs, and the optical delay can be changed by moving of mirror's position from zero to 25 nanoseconds.

higher energy input to a microvolume is reached and electron gas pressure can overcome GPa for liquids and TPa for solids [8, 9, 13–15] and as a result, an extreme state of matter is formed. Due to such huge pressure, supersonic shock waves are emitted from the plasma formation region. The shape and initial speed of the shock wave strongly depend on the spatial laser-plasma density distribution. To control the shock wave one, a special complex pattern of laser-induced plasma can be created. One of the possible ways to create such a specific pattern is by adding aberrations to the optical scheme, enabling non-uniform shock wave generation in water [16]. The strongly non-spherical shock wave can be a useful tool in the synthesis of new materials [17], 3D microfluidic chip fabrication [18], phase separation, new unusual phase transition [4], chemical reaction control [19] and a variety of medical therapies such as mechanical optical clearing [16].

In this letter, we report the first, to our knowledge, *in situ* space-time characterization of shock wave changes induced by a femtosecond laser-plasma filament in water as a convenient prototype for a condensed medium. We focus on a study of features controlling the parameters of the shock wave produced in water by a tightly focused femtosecond laser beam with a power significantly exceeding critical power (up to $50P_{cr}$). Two major points, namely tight focusing (numerical aperture (NA) = 0. 4) and significant overcoming of the critical power, provide a unique single filament generation regime with close to critical electron density value along its axis, which cannot be reached in other cases. This provides the advantage of increased control over the properties and geometry of the laser-induced shock waves in a liquid sample. Moreover, we discuss the aberrations as one of the possible ways to effectively increase the filament length and shock impact of the material.

2. Experimental setup

In the experiments the Cr:forsterite femtosecond laser (wavelength of 1240 nm, pulse duration of about 140 fs, laser energy up to 150 μJ, intensity contrast of about 5×10^4 ASE and repetition rate of 10 Hz) was employed. A shadow photography technique was applied to probe the dynamics of laser-induced shock waves. In this technique, shadows of the shock waves as well as cavitation bubbles were observed on the charge-coupled device (CCD) camera due to probe pulse scattering on the refractive index modulations, caused by the acoustic pressure. The experimental scheme is sketched in figure 1.

A beam splitter divided the initial laser beam into two beams: pump and probe. The half-wave plate with a Glan prism was used for attenuation of the incident pulse energy. The pump beam was tightly focused into a water cell (wall width of 100 μm) by two different aspheric lenses manufactured by Philips (for CAY033, the NA was 0.4 and the focal length was 3.3 mm; for CAY046 the NA was 0.4 and the focal length was 4.6 mm). The different lenses were selected to realize different regimes of plasma formation. For the CAY033 lens, the focal spot diameter was 4 μm and the Rayleigh length was 15 μm measured in air conditions. Taking into account linear absorption of water at 1240 nm at about 1.16 cm^{-1}, only 61% and 50% of incoming energy was delivered to the focal waist in case of CAY033 and CAY046 lenses, respectively. For visualization on a CCD camera the frequency of the probe pulse was doubled in a beta barium borate (BBO) crystal. Then, the probe beam was scattered by a diffuser plate for uniform illumination of the water cell and then collected by the CCD camera. The optical delay could be changed by moving the mirror's position from zero to 25 nanoseconds. Turning the focusing lens at 180° with respect to laser radiation allowed us to artificially add spherical aberrations to the scheme. To characterize focusing conditions, the experiments were carried out in air and in water. When the aspheric lens was placed in air, a bright spark 4 μm in diameter and about 30 μm in length was observed. However, in water, a plasma channel (length more than 100 μm) was formed. To avoid aberrations in other cases, the aspheric lens was placed inside the water cell.

Examples of the shadowgrams are provided in figure 2. To improve image quality, ten images were averaged and the background was subtracted. Using this technique, we observed the shock wave dynamics on a nanosecond timescale. It is

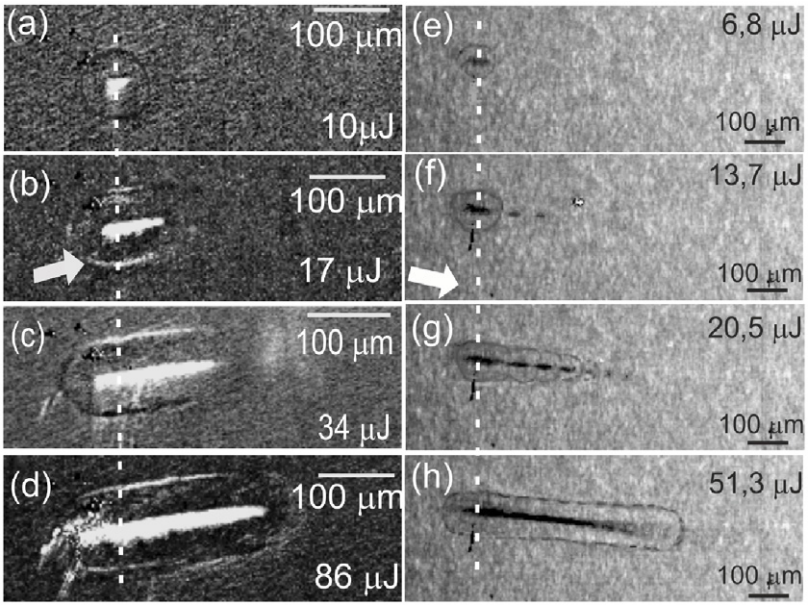

Figure 2. The shadowgrams of the shock waves, delayed on 18.6 ns. The incident laser pulse energy: (*a*) 10, (*b*) 17, (*c*) 34, (*d*) 86, (*e*) 6.6, (*f*) 13.7, (*g*) 20.5 and (*h*) 51.3 μJ. The shadow pictures in the left column were observed when a 3.3 mm focusing lens was used. The bright region in the centre shows the plasma location. The contour outside the plasma region shows the laser-induced shock wave front. The shadow photographs on the right were observed when the aberrations were added to the scheme using a 4.6 mm focusing lens. In addition, a bandpass (620 ± 20 nm) filter for plasma radiation blocking was added to the scheme. The dark regions show the cavitation area and shock waves.

well known that there is a threshold of shock wave formation that can serve as an ionization breakdown indicator. The laser energy of the shock wave formation threshold was measured as 6 ± 1 μJ from the shadow pictures captured for the lens with 3.3 mm focusing length. Taking into account linear absorption, the ionization breakdown threshold was equal to 3.6 ± 0.2 μJ (the laser intensity was about 10^{13} W cm^{-2}). This is in a good agreement with results obtained by other methods using similar focusing geometry, both in water and in other transparent dielectrics [20].

For contrast shock wave creation, it is necessary to deliver extreme energy to a microvolume. In the case of loosely (NA less than 0.2) focused or collimated beams, the simple increase of laser radiation power fails to achieve high plasma densities. When the peak power of the laser radiation is significantly higher (supercritical regime, P ~50 P_{cr}) than the critical power of self-focusing [1], a dynamic balance between self-focusing, plasma defocusing, and diffraction occurs and thus a laser filament is formed. In this case, at such high peak powers of laser radiation, small-scale self-focusing results in the laser beam falling into multiple thread-like, separate living filaments [21]. The electron density in each filament is about 10^{18} cm^{-3} [8]. Thus, the pressure, achieved in the ideal electron gas at such densities and electron energies (about several eV), is about several kilobars ($p = n_e$ kT). For such low shock pressures the speed of shock waves are slightly above the speed of sound and shock wave's amplitude is low. Consequently, such shock waves are not detectable by the shadow photography technique since the modulation of the refractive index is proportional to the shock wave amplitude. Our preliminary experiments in loose focusing conditions showed that in the regime of multiple filamentation there were no detectable cavitation bubbles and laser-induced shock waves. For 0.2 < NA < 0.3, energy localization along the optical axis grows and competition occurred with a strong energy exchange between different filaments [1, 21]. This led to random filament distribution across the laser beam and each filament launches a shock wave; however, they did not form one contrast wave. In case of tight focusing geometry (NA ≥ 0, 3), electron density was about 0,1n_{cr} ($n_{cr} = m_e\omega^2/4\pi e^2 \cong 7.3 \times 10^{20}$ cm^{-3}) and the plasma electron energy was sufficiently larger than in loose focusing geometry [13]. The electron gas pressure in this case was about 1 GPa, which led to contrast shock wave generation. In this regime, the energy was localized in the microvolume that is 4 μm in diameter and thus there are no conditions for the multiple filamentation; as a result, a single continuous filament was created [6, 16]. The length of the femtosecond filament depends on the energy absorbed from the laser pulse. Increasing the energy of the laser pulse leads to an increase in the length of the filament. This growth is limited by linear and nonlinear absorption in medium. Varying the energy of the laser pulse, we determined two different regimes. At energies slightly above the threshold, one spherical shock wave is formed (see figure 3(*a*)). With the increase of laser pulse energy, a single, stable pulse-to-pulse laser filament is fired. Each point of the filament becomes the centre of shock wave and cavitation bubble generation. The superposition of these spherical shock waves builds the cylindrical shock wave [22]. Shock wave diameter evolution with the laser energy can be restored from shadow pictures (see figure 3). The subsequent shock wave dynamics can be completely described by hydrodynamic equations [23].

In the experiments, we determined that shock wave diameter tends to saturation with the square root of incident pulse

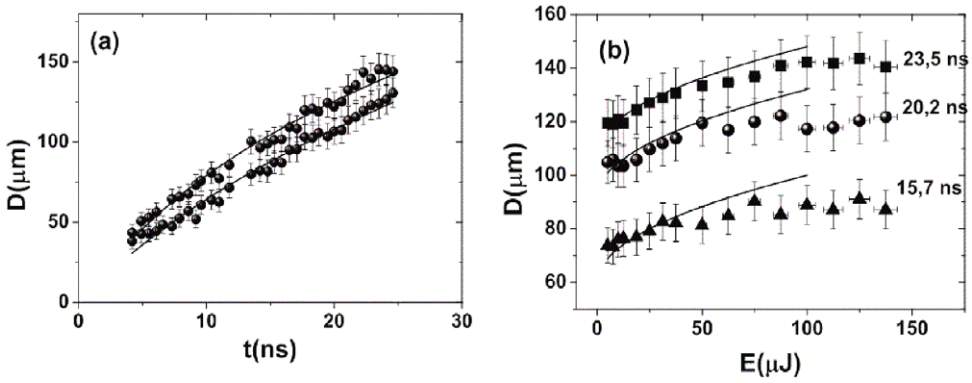

Figure 3. (*a*) The shock wave leading and trailing edge diameters D as a function of the time delay. The laser energy is equal to 130 μJ. Lines show an approximation with shock wave velocity exponential decay. (*b*) The shock wave diameter D as a function of the laser pulse energy E. Three series of experimental data were measured at time delays equal to 15.7, 20.2 and 23.5 ns. The lines show the square root dependence.

energy (see figure 3(*b*)). This can be explained if intensity clamping is taken into account. With the increase of laser pulse energy, the intensity tends to saturation due to the dynamic balance process taking place in the laser filament. Therefore, there is a plateau in the electron concentration [24]. Thus, the energy that can be transferred from the laser radiation to the plasma and then from the plasma to each shock wave in the ionization breakdown volume is limited. For femtosecond pulses, the role of plasma shielding is less than in the cases where picosecond or nanosecond pulses are used because the plasma is formed at the tail of the femtosecond pulse and effective shielding cannot be achieved [25]. The shock wave energy is the square root of its radius, due to the mass flow conservation and its spherical symmetry [26].

Using the experimental dependence of diameter of the shock wave on time, it is easy to estimate shock wave front velocity. In the simplest case, speed decreases exponentially, reducing to the speed of sound [27]. To estimate pressure at the shock front, an empirical equation was used [28]. For the incident laser energy of 130 μJ, the shock wave front velocity is 2300 $\pm$ 200 m s^{-1}. The shock pressure can be calculated as 1.0 $\pm$ 0.1 GPa, which is similar to the results in [27, 29, 30] and in good agreement with shock pressure upper limits corresponding to the electron gas pressure estimated by 1 GPa for a density value of 0,1 n_{cr} and the electron mean energy about 10 eV.

The last series of experiments were carried out with a CAY046 lens when aberrations were added to the optical scheme. The aberrations provide an opportunity to create a hot spot complex pattern along the optical axis. The intensity of the laser radiation decreases with each following hot spot [31]. In this regime, multiple shock waves are generated. Aberration hot spots become the centres for cavitation bubbles and spherical shock wave generation. At low laser pulse energies, only spherical shock waves are generated (see figure 2(*e*)). At higher laser pulse energies, several dotted sources, isolated from each other, create a complex envelope of shock waves (see figure 2(*f*), (*g*) [22]). With the increase of laser energy, additional shock waves are generated from new plasma, forming a cylindrical shock wave (see figure 2(*h*)). This is caused by filament formation in each hot spot. The phenomenon is similar to one observed by using a lens with a 3.3 mm focusing length. Thus, aberrations could effectively increase the length of the laser filament and the laser-induced shock impact on material.

3. Conclusion

We performed the first spatio-temporally resolved study of shock wave changes induced by femtosecond laser-plasma filament in water in a supercritical power regime. Laser-driven plasma assisted shock wave shaping by varying the femtosecond laser pulse energy and focusing parameters was carried out. It was shown that tight focusing of an intense femtosecond laser beam provides the unique opportunity to fire a single steady filament in a liquid sample. Redistribution of the energy conserved in the filament on a nanosecond time scale leads to contrast laser-induced shock wave generation. The parameters of such laser-induced shock waves can be easily controlled and cannot be realized in a multifilament regime. Only at the specific threshold energy were spherical shock waves generated. With the increase of laser pulse energy, multiple spherical shock waves were generated, forming a single cylindrical shock wave. Aberrations added to the optical scheme lead to multiple dotted plasma sources for shock wave formation, spaced along the axis of pulse propagation. Increasing the laser energy launches at each dot enhances the length of the entire filament and as a result, the shock impact on the material. In the plasma assisted regime, the dependence of the diameter of the cylindrical shock wave on laser pulse energy tends to saturation, which can be associated with intensity clamping (saturation) in the laser filament. The profile of the laser-induced shock wave is non-uniform; therefore, when aberrations are added to the optical scheme, complex patterns of non-spherical shock wave can be generated.

Acknowledgements

The authors wish to thank Irina Zhvania for drawing the experimental setup and Eugenie Smetanina for fruitful discussions. This research has been supported by the Russian

Foundation for Basic Research (Project No. 14-02-00819a) and partly by the M.V. Lomonosov Moscow State University Program of Development.

References

[1] Couairon A and Mysyrowicz A 2007 Femtosecond filamentation in transparent media *Phys. Rep*. **441** 47–189

[2] Venugopalan V, Iii A G, Nahen K and Vogel A 2002 Role of laser-induced plasma formation in pulsed cellular microsurgery and micromanipulation *Phys. Rev. Lett.* **88** 078103

[3] Kiran P P, Bagchi S, Arnold C L, Krishnan S R, Kumar G R and Couairon A 2010 Filamentation without intensity clamping *Opt. Express* **18** 21504–10

[4] Mizeikis V, Vailionis A, Gamaly E G, Yang W, Rode A V and Juodkazis S 2012 Synthesis of super-dense phase of aluminum under extreme pressure and temperature conditions created by femtosecond laser pulses in sapphire ed W V Schoenfeld, R C Rumpf and G von Freymann *Proc. SPIE* **8249** 82490A

[5] Luo L, Wang D, Li C, Jiang H, Yang H and Gong Q 2002 Formation of diversiform microstructures in wide-bandgap materials by tight-focusing femtosecond laser pulses *J. Opt. A: Pure Appl. Opt*. **4** 105–10

[6] Dergachev A A, Ionin A A, Kandidov V P, Seleznev L V, Sinitsyn D V, Sunchugasheva E S and Shlenov S A 2013 Filamentation of IR and UV femtosecond pulses upon focusing in air *Quantum Electron*. **43** 29–6

[7] Franjic K and Miller D 2010 Vibrationally excited ultrafast thermodynamic phase transitions at the water/air interface *Phys. Chem. Chem. Phys*. **12** 5225–39

[8] Minardi S, Gopal A, Tatarakis M, Couairon A, Tamosauskas G, Piskarskas R, Dubietis A and Di Trapani P 2008 Time-resolved refractive index and absorption mapping of light-plasma filaments in water *Opt. Lett*. **33** 86–8

[9] Babin A A, Kiselev A M, Kulagin D I, Pravdenko K I and Stepanov A N 2004 Shock-wave generation upon axicon focusing of femtosecond laser radiation in transparent dielectrics *J. Exp. Theor. Phys. Lett*. **80** 298–2

[10] Couairon A, Sudrie L, Franco M, Prade B and Mysyrowicz A 2005 Filamentation and damage in fused silica induced by tightly focused femtosecond laser pulses *Phys. Rev.* B **71** 125435

[11] Gamaly E G 2011 The physics of ultra-short laser interaction with solids at non-relativistic intensities *Phys. Rep*. **508** 91–243

[12] Liu X-L, Lu X, Liu X, Xi T-T, Liu F, Ma J-L and Zhang J 2010 Tightly focused femtosecond laser pulse in air: from filamentation to breakdown. *Opt. Express* **18** 26007

[13] Liu W, Kosareva O, Golubtsov I S, Iwasaki A, Becker A, Kandidov V P and Chin S L 2003 Femtosecond laser pulse filamentation versus optical breakdown in H2O *Appl. Phys. B Lasers Opt*. **76** 215–29

[14] Wahlstrand J K, Jhajj N, Rosenthal E W, Zahedpour S and Milchberg H M 2014 Direct imaging of the acoustic waves generated by femtosecond filaments in air *Opt. Lett*. **39** 1290

[15] Potemkin F V, Mareev E I, Mikheev P M and Khodakovskij N G 2013 Resonant laser-plasma excitation of coherent THz phonons under extreme conditions of femtosecond plasma formation in a bulk of fluorine-containing crystals *Laser Phys. Lett*. **10** 076003

[16] Lauterborn W and Vogel A 2013 *Bubble Dynamics and Shock Waves* ed C F Delale (Berlin, Heidelberg: Springer)

[17] Vailionis A, Gamaly E G, Mizeikis V, Yang W, Rode A V and Juodkazis S 2011 Evidence of superdense aluminium synthesized by ultrafast microexplosion *Nat. Commun*. **2** 445

[18] Li Y and Qu S 2013 Water-assisted femtosecond laser ablation for fabricating three-dimensional microfluidic chips *Curr. Appl. Phys*. **13** 1292–5

[19] Thadhani N N 1994 Shock-induced and shock-assisted solid-state chemical reactions in powder mixtures *J. Appl. Phys*. **76** 2129

[20] Gordienko V M, Makarov I A, Mikheev P M, Savel'ev A B, Shashkov A A and Volkov R V 2004 Self-channeling of femtosecond laser radiation in transparent two-component condensed medium ed V P Veiko *Proc. SPIE* **5399** 96–9

[21] Abraham E, Minoshima K and Matsumoto H 2000 Femtosecond laser-induced breakdown in water : time-resolved shadow imaging and two-color interferometric imaging *Opt. Commun*. **176** 441–52

[22] Steiner H, Gretler W and Hirschler T 1998 Numerical solution for spherical laser-driven shock waves *Shock Waves* **8** 139–47

[23] Leela C, Bagchi S, Kumar V R, Tewari S P and Kiran P P 2013 Dynamics of laser induced micro-shock waves and hot core plasma in quiescent air *Laser Part. Beams* **31** 263–72

[24] Mikheev P M and Potemkin F V 2011 Generation of the third harmonic of near IR femtosecond laser radiation tightly focused into the bulk of a transparent dielectric in the regime of plasma formation *Moscow Univ. Phys. Bull*. **66** 19–24

[25] Boppart S A, Toth C A, Roach W P and Rockwell B A 1993 Shielding effectiveness of femtosecond laser-induced plasmas in ultrapure water *SPIE Laser-Tissue Interact. IV* **1882** 347–54

[26] Kennedy P K, Hammer D X and Rockwell B A 1997 Laser-induced breakdown in aqueous media *Prog. Quantum Electron*. **21** 155–248

[27] Devia-Cruz L F, Camacho-López S, Evans R, García-Casillas D and Stepanov S 2012 Laser-induced cavitation phenomenon studied using three different optically-based approaches—an initial overview of results *Photon. Lasers Med*. **1** 195–5

[28] Vogel A, Busch S and Parlitz U 1996 Shock wave emission and cavitation bubble generation by picosecond and nanosecond optical breakdown in water *J. Acoust. Soc. Am*. **100** 148–65

[29] Schaffer C, Nishimura N, Glezer E, Kim A and Mazur E 2002 Dynamics of femtosecond laser-induced breakdown in water from femtoseconds to microseconds. *Opt. Express* **10** 196–203

[30] Strycker B D, Springer M M, Traverso A J, Kolomenskii A A, Kattawar G W and Sokolov A V 2013 Femtosecond-laser-induced shockwaves in water generated at an air–water interface *Opt. Express* **21** 23772–84

[31] Marcinkevičius A, Mizeikis V, Juodkazis S, Matsuo S and Misawa H 2003 Effect of refractive index-mismatch on laser microfabrication in silica glass *Appl. Phys. A Mater. Sci. Process.* **76** 257–60